1521-009X/49/4/305–313$35.00
Drug Metabolism and Disposition

https://doi.org/10.1124/dmd.120.000275
Drug Metab Dispos 49:305–313, April 2021

Functional Proliferating Human Hepatocytes: In Vitro Hepatocyte Model for Drug Metabolism, Excretion, and Toxicity[S]

Shida Qiao,[1] Sisi Feng,[1] Zhitao Wu, Ting He, Chen Ma, Zhaoliang Peng, E. Tian, and Guoyu Pan

Shanghai Institute of Materia Medica, Chinese Academy of Sciences, Shanghai, China (S.Q., Z.W., C.M., Z.P., G.P.); University of Chinese Academy of Sciences, Beijing, China (S.Q., Z.W., C.M., Z.P., G.P.); Shanghai Hexaell Biotech Co., Ltd, Shanghai, China (S.F., E.T.); Nanjing University of Chinese Medicine, Nanjing, China (Z.W.); and Nanjing Tech University, Nanjing, China (T.H.)

ABSTRACT

To develop a functional alternative hepatocyte model for primary human hepatocytes (PHHs) with proliferative property, essential drug metabolic, and transporter functions, proliferating human hepatocytes (ProliHHs) expanded from PHHs were fully characterized in vitro. Herein, ProliHHs generated from multiple PHHs donors could be expanded more than 200-fold within four passages and maintained their metabolic or transporter capacities partially. Furthermore, ProliHHs were able to regain the mature hepatic property after three-dimensional (3D) culture. Particularly, the downregulated mRNA expression and function of three major cytochrome P450 (P450) enzymes (CYP1A2, CYP2B6, and CYP3A4) in the proliferating process (ProliHHs-P) could be recovered by 3D culture. The metabolic variabilities across different PHHs donors could be inherited to their matured ProliHHs (ProliHHs-M). The intrinsic clearances of seven major P450 enzymes in ProliHHs-M correlated well (r = 0.87) with those in PHHs. Also, bile canaliculi structures could be observed in sandwich-cultured ProliHHs (SC-ProliHHs), and the biliary excretion index of four probe compounds [cholyl-lys-fluorescein, 5-(and-6)-carboxy-2′, 7′-dichlorofluorescein diacetate (CDF), deuterium-labeled sodium taurocholate acid, and rosuvastatin] in SC-ProliHHs (>10%) were close to sandwich-cultured PHHs. More importantly, both ProliHHs-P and ProliHHs-M could be used to evaluate hepatotoxicity. Therefore, these findings demonstrated that the 3D and sandwich culture system could be used to recover the metabolic and transporter functions in ProliHHs for clearance prediction and cholestasis risk assessment, respectively. Together, ProliHHs could be a promising substitute for PHHs in drug metabolism, transport, and hepatotoxicity screening.

SIGNIFICANCE STATEMENT

This report describes the study of drug metabolic capacities, efflux transporter functions, and toxicity assessments of proliferating human hepatocytes (ProliHHs). The metabolic variability in different primary human hepatocyte donors could be inherited by their matured ProliHHs derivatives. Also, ProliHHs could form canalicular networks in sandwich culture and display biliary excretion capacities. More importantly, both the proliferative and maturation statuses of ProliHHs could be used to evaluate hepatotoxicity. Together, ProliHHs were feasible to support drug candidate screening in hepatic metabolism, disposition, and toxicity.

Introduction

Assessments of drug metabolism, transport, and hepatotoxicity are essential parts of early drug discovery (Godoy et al., 2013; Zhang et al., 2016). Primary human hepatocytes (PHHs) have been widely recognized as the gold standard for predicting drug clearance and hepatotoxicity (Gómez-Lechón et al., 2003, 2004; Hewitt et al., 2007). However, the loss of character, including proliferative properties and metabolic and transported functions of PHHs after in vitro culture, limits their applications (Gómez-Lechón et al., 2003; O'Brien et al., 2006). Moreover, it is time consuming and costly to determine the variabilities of drug-metabolizing enzymes (DMEs) and transporters from different PHHs batches (Donato et al., 2013). Therefore, the establishment of a functional substitutable hepatocyte model is an important issue.

Significant efforts have been made in the past decade. In addition to PHHs, embryonic stem cell–derived, induced pluripotent stem cell–derived, or epigenetic reprogramming–induced hepatocyte technology was developed to solve the lack of donors. However, a better differentiation protocol was still missing to generate physiologically relevant hepatocytes (Brolén et al., 2010; Si-Tayeb et al., 2010; Ogawa et al., 2013; Huang et al., 2014). Also, there are several investigations

This study was supported by the "Organ Reconstruction and Manufacturing" Strategic Priority Research Program of the Chinese Academy of Sciences [Grant XDA16020205], the National Science Foundation of China [Grant 81872927], the International Partnership Program of Chinese Academy of Sciences [Grant 153631KYSB20160004], the Independent Deployment Program of the Institute of Pharmaceutical Innovation of the Chinese Academy of Sciences [Grant CASIMM0120184005], and the China Postdoctoral Science Foundation [Grant 2019M651623].

[1]S.Q. and S.F. contributed equally to this work.

https://doi.org/10.1124/dmd.120.000275.

[S]This article has supplemental material available at dmd.aspetjournals.org.

ABBREVIATIONS: AAFE, absolute average fold error; BEI, biliary excretion index; BSEP, bile salt export pump; CDFDA, 5-(and-6)-carboxy-2′, 7′-dichlorofluorescein diacetate; CLF, cholyl-lys-fluorescein; CL_{int}, intrinsic clearance; 2D, two-dimensional; 3D, three-dimensional; DILI, drug-induced liver injury; DME, drug-metabolizing enzyme; DMEM, Dulbecco's modified Eagle's medium; d8-TCA, deuterium-labeled sodium taurocholate acid; HBSS, Hanks' balanced salt solution; HIM, hepatic maturation medium; MRP2, multidrug resistance-associated protein 2; P450, cytochrome P450; PHH, primary human hepatocyte; ProliHHs, proliferating human hepatocytes; ProliHHs-M, maturation status of ProliHHs; ProliHHs-P, proliferative status of ProliHHs; PS, penicillin-streptomycin; qPCR, quantitative polymerase chain reaction; SC-PHHs, sandwich-cultured PHHs; SC-ProliHHs, sandwich-cultured ProliHHs; SC-ProliHHs-M, sandwich-cultured ProliHHs-M; SC-ProliHHs-P, sandwich-cultured ProliHHs-P; TC_{50}, median toxic concentration; UHH, Upcyte human hepatocyte; WME, Williams' medium E.

about reprogramming PHHs into hepatic progenitor cells to obtain cell proliferation features and maintain physiologically relevance, but these proliferative cells lose mature hepatic features quickly and have not been widely used in drug toxicity screening (Kim et al., 2018; Fu et al., 2019). Moreover, multiple reports on applications of HepaRG cells and Upcyte human hepatocytes (UHHs) in metabolic and toxicological evaluation were published (Andersson et al., 2012; Levy et al., 2015; Ramachandran et al., 2015). However, to the best of our knowledge, different clones, passages, and differentiation protocols in HepaRG cells may lead to poor repeatability (Petrov et al., 2018); the transcriptional levels of major cytochrome P450 (P450) enzymes in UHHs are still to be improved at donor-specific levels, and the efflux transporter functions for biliary excretion were not reported (Levy et al., 2015; Schaefer et al., 2016). Furthermore, genetic manipulation by overexpressing human papillomavirus genes (E6 and E7) or other immortal genes is not the best way to obtain expanded hepatocytes with genomic instability (Liang and Zhang, 2013; Ma et al., 2014).

Recently, the development of dedifferentition strategy, a breakthrough in developing an in vitro surrogate hepatocyte model for PHHs, made it feasible for PHHs to expand as proliferating human hepatocytes (ProliHHs), which can be matured in a three-dimensional (3D) culture environment (Zhang et al., 2018). Unlike other dedifferentiation strategies for PHHs, ProliHHs are biphenotypic, partially maintaining mature hepatocyte features and gaining expression of progenitor-associated genes. Compared with human pluripotent stem cell–derived hepatocytes and human induced hepatocytes, ProliHHs show promising potential for in vitro drug safety assessment because of expression of transporter and activity of CYP2B6 (Zhang et al., 2018). However, it is still unclear whether ProliHHs can feasibly predict drug hepatic clearance, biliary excretion, and hepatotoxicity in vitro.

In this study, we generated ProliHHs from different PHHs donors. Three major DMEs' expression and function in ProliHHs were systematically characterized, and the relevance of seven major DMEs was then investigated between the maturation status of ProliHHs (ProliHHs-M) and PHHs. After sandwich culture, cell polarization and efflux transporter function were identified in ProliHHs. Also, cytotoxicity induced by selected compounds was tested in ProliHHs. Together, these results suggested that ProliHHs can be an alternative hepatocyte model for PHHs in drug metabolism, transport, and hepatotoxicity screening.

Materials and Methods

Chemicals and Reagents. Phenacetin, bupropion, testosterone, chlorzoxazone, diclofenac acid, *S*-mephenytoin, dextromethorphan, dexamethasone, *N*-acetyl-cysteine, human [leu15]-gastrin I, penicillin-streptomycin (100×), 3-(4,5-dimethylthiazol-2-yl)-2,5-diphenyltetrazolium bromide, chir99021, ibuprofen, lithocholic acid, chenodeoxycholic acid, chlorpromazine, cyclosporin A, rifampin, troglitazone, tamoxifen, amiodarone, imipramine, isoniazid, valproic acid, rosuvastatin, glibenciamide, and ketoconazole were purchased from Sigma-Aldrich (St. Louis, MO). Advanced Dulbecco's modified Eagle's medium (DMEM)/Ham's F-12, DMEM, Williams' medium E (WME), Hanks' balanced salt solution (HBSS), FBS, ITS^{TM+} Premix (insulin, transferrin, selenium), and 0.25% trypsin-EDTA were purchased from Invitrogen (Carlsbad, CA). Recombinant human epidermal growth factor, recombinant human hepatocyte growth factor, oncostatin M, and recombinant human fibroblast growth factor 10 were purchased from PeproTech (Rocky Hill, NJ). Cholyl-lys-fluorescein (CLF) and 5-(and-6)-carboxy-2′, 7′-dichlorofluorescein diacetate (CDFDA) were purchased from AAT Bioquest (Sunnyvale, CA). Deuterium-labeled sodium taurocholate (d8-TCA) was purchased from GIBCO (Carlsbad, CA).

The Culture of PHHs. Cryopreserved PHHs were purchased from BioreclamationIVT (Baltimore, MD) and XenoTech (Lenexa, KS). The human hepatocytes' donor information is presented in Supplemental Table 1. Briefly, the cryopreserved PHHs were resuscitated and suspended following vendor's recommendations. PHH cells were diluted to 3.5×10^5 cells per well and plated onto 24-well plates, coated with collagen I in plating medium [WME supplemented with 1 μM dexamethasone, 5% FBS, and 1% penicillin-streptomycin (PS)]. Attached PHHs were maintained in feeding medium (WME supplemented with 1× ITS^{TM+} Premix, 0.1 μM dexamethasone, 1% FBS, and 1% PS), and feeding medium was changed every day (Pan et al., 2012).

The Derivation and Proliferation of ProliHHs from PHHs. Cryopreserved PHHs were firstly seeded at required density (5×10^5 cells/well) in a six-well plate, coated with collagen I and cultured under hypoxia conditions (5% O_2, 5% CO_2, 37°C) (Zhang et al., 2018). To obtain proliferative status of ProliHHs (ProliHHs-P), plating medium was replaced with HM medium (HM, advanced DMEM/Ham's F-12 supplemented with 10 μM Y-27632, 5 μM A83-01, 50 ng/ml Wnt3a protein, or 5 μM chir99021, 2 ng/ml recombinant human fibroblast growth factor 10, 50 ng/ml recombinant human epidermal growth factor, 25 ng/ml recombinant human hepatocyte growth factor, 10 nM Human [Leu15]-gastrin I, 1× N2 supplement 100×, 1 mM N-acetyl-cystein, 1× B27 supplement 50× minus vitamin A, 1% FBS, 10 mM nicotinamide, and 1% PS) within 10–24 hours after PHHs seeding, and the HM medium was changed every 2 days. For monolayer expansion, ProliHHs were seeded at six-well plate (1×10^5 cells/well) under hypoxia condition and trypsinized at day 7 for passaging. The HM medium was changed every 2 days.

The Maturation of ProliHHs in 3D Culture System. For rapid hepatic maturation, ProliHHs were seeded at 2.5×10^5 cells per well and aggregated in an Ultra-Low Attachment 24-well plate (Kuraray, Corning, Tewksbury, MA) and formed spheres in hepatic maturation medium (HIM; HM supplemented with 5 μM forskolin, 1 μM dexamethasone, 20 ng/ml oncostatin M) under normoxia condition (5% CO_2 incubator). A 50% HIM was then exchanged daily to allow further maturation for about 7–10 days. These ProliHHs-M were further used in P450 metabolic assay or sandwich culture.

The Sandwich Culture of ProliHHs. For sandwich culture, trypsinized ProliHHs (3.5×10^5 cells/well) from proliferative or maturation status were seeded onto collagen I–coated 24-well plates. ProliHHs were incubated overnight, and HIM was renewed. Attached ProliHHs were overlaid with 0.25 mg/ml Matrigel in HIM and incubated under normoxia condition (5% CO_2 incubator) to form sandwich configuration. Sandwich-cultured ProliHHs were further used in CDFDA staining and biliary excretion measurement at day 7.

Phase Microscopy Imaging. Hepatocyte morphology was assessed using phase-contrast microscopy to ensure healthy optimal culture for experiments. ProliHHs-P and PHHs were monitored on a daily basis. The images of ProliHHs-P were recorded on days 1, 7, 14, and 28. ProliHHs-M were recorded on days 1, 3, and 7 to recheck the sphere stage. Sandwich-cultured PHHs (SC-PHHs) were recorded and checked on days 1 and 5 to ensure bile canaliculi formation. Sandwich-cultured ProliHHs (SC-ProliHHs) were recorded and checked at days 1 and 7.

RNA Isolation and Real-Time Quantitative Polymerase Chain Reaction. Total RNA extracted from ProliHHs and PHHs was isolated from TRIzol reagent (Invitrogen). The cDNA was transcribed by 1000 ng total RNA with a Primescript RT Reagent Kit (Takara, Tokyo, Japan). Real-time quantitative polymerase chain reaction (qPCR) was performed with a real-time qPCR kit (Yeasen, Shanghai, China) and SYBR Green Master Mix (Yeasen) on Applied Biosystems 7500 (Applied Biosystems, Foster City, CA). Primers are listed in Supplemental Table 2.

Measurement of Human Albumin Levels. For ProliHHs-P and PHHs, supernatants were collected from six-well plate when cells were attached to the plate at day 1. For ProliHHs-M, supernatants were collected from 24-well plate at day 0 (trypsinized from ProliHHs-P), day 2, and day 8. Human albumin ELISA Quantitation Set was purchased from Bethyl Laboratory (Montgomery, TX) and used to measure human albumin secretion level.

P450 Metabolic Capacity Determination. Clearance of probe compounds was determined at designated time points (day 7, passage 4 in ProliHHs-P and day 7 in ProliHHs-M). For measurement of activities of three major DMEs (CYP1A2, CYP2B6 and CYP3A4), ProliHHs-P (5×10^5 cells/well) and PHHs (1×10^5 cells/well) were seeded in a 24-well plate. For the measurement of seven metabolic activities of P450 enzymes, ProliHHs-M were seeded at 2.5×10^5 cells per well and cultured in a 24-well Ultra-Low Attachment plate in HIM for 7 days. ProliHHs and PHHs were incubated in 1 ml medium with probe substrates listed in Supplemental Table 3. The supernatants (100 μl) were collected from PHHs,

ProliHHs-P, and ProliHHs-M at 0, 1, 2, and 3 hours after administration of substrate. The metabolic assay was stopped by adding 300 μl ice-cold acetonitrile. The probe compounds were analyzed by LCMS-8030 (Shimadzu, Kyoto, Japan). Drug clearance was determined through parent compound disappearance rate as follows:

$$Elimination\ rate\ constant\ (k) = (-gradient)$$

$$Half\ life\ (t_{1/2})(minutes) = \frac{0.693}{k}$$

$$V(\mu l/million\ cells) = \frac{Incubation\ volume(\mu l)}{Number\ of\ cells\ in\ incubation\ (\times 10^6)}$$

$$Intrinsic\ Clearance\ (CL_{int})\ (\mu l/min\ per\ million\ cells) = \frac{0.693\ \times\ V}{t_{1/2}}$$

Hepatocyte Polarization and Biliary Excretion Capacity Measurement Assay. ProliHHs-P, ProliHHs-M, and PHHs were seeded at required density (3.5×10^5 cells/well) in 24-well plates. The formation of bile canaliculi networks in polarized hepatocytes were visualized by CDFDA (Levy et al., 2015). Generally, 5 mM stock CDFDA solution 1:500 was diluted in culture medium and incubated at 37°C for 30 minutes in the dark to detect the hepatocyte polarization. To measure the efflux transporter activities of ProliHHs and PHHs, different transporter substrates were selected: CLF [bile salt efflux pump (BSEP)], CDF [multidrug resistance-associated protein 2 (MRP2)], d8-TCA (BSEP), and rosuvastatin (MRP2). Biliary excretion index (BEI) values were determined over a 15-minute interval after preincubation with warm HBSS with or without Ca^{2+} (Liu et al., 1999). For PHHs, the BEI study was performed on day 5. The fluorescence intensity of CDF and CLF in sandwich-cultured ProliHHs or PHHs were measured at excitation/emission wavelengths of 495/529 and 492/536 nm, respectively. According to our previous report protocol, the concentration of d8-TCA and rosuvastatin in sandwich-cultured ProliHHs or PHHs was analyzed by LCMS-8030 (Shimadzu) (Pan et al., 2012; Guo et al., 2014).

The BEI value was calculated as follows:

$$BEI = \left(1 - \frac{A_{minus\_Ca++}}{A_{plus\_Ca++}}\right) \times 100\%$$

A was the concentration or amount of test compound accumulated in the absence (A_{minus_Ca++}) or presence (A_{plus_Ca++}) of Ca^{2+}, which was achieved through adding warm Ca^{2+}-free or standard HBSS buffer (Wu et al., 2016).

In Vitro Cytotoxicity Assay. ProliHHs-P and PHHs were seeded at required density (3×10^4 cells/well) in collagen I–coated 96-well plates. The medium containing test compounds were replaced in each well after cells attached and then incubated 24 hours. For ProliHHs-M spheroids in toxicity testing, 1.5% agarose–coated 96-well plates stored at 4°C were prepared prior to ProliHHs seeding. ProliHHs were then seeded at required density (3×10^4 cells/well) in agarose-coated 96-well plates to form spheres, and 50% HIM was changed every other day. At the fifth day, tested compounds were replaced and incubated for 24 hours in ProliHHs-M. Cell viability was measured by Cell Counting Kit 8 (Yeasen) or 3-(4,5-dimethylthiazol-2-yl)-2,5-diphenyltetrazolium bromide assay.

Statistical Analysis. All data were expressed as means ± S.D. unless otherwise stated using GraphPad Prism 5.0 software (GraphPad Software Inc., La Jolla, CA). Unpaired *t* test and one-way ANOVA were used to analyze comparisons of two and more than two groups, respectively. Correlations were calculated using Pearson correlation coefficient. In all analyses, a difference was considered as significant: *P* value <0.05, *P* value <0.01, and *P* value <0.001. The intrinsic clearance (CL_{int}) and median toxic concentration (TC_{50}) value in ProliHHs were compared with the observed values in PHHs to determine the predictability using absolute average fold error (AAFE), and AAFE value was calculated by the following equation (Kimoto et al., 2017):

$$AAFE = 10^{\frac{1}{N}\sum\left|\log_{10}\frac{ProliHH}{PHH}\right|}$$

Results

Generation, Maturation, and Cultured Characteristics of ProliHHs. The generation and maturation strategies are illustrated in Fig. 1A. ProliHHs in proliferative or maturation status [two-dimensional (2D) or 3D cultured] are abbreviated as ProliHHs-P or ProliHHs-M, respectively. In this study, with the help of HM medium and hypoxia culture conditions, PHHs started to proliferate and gradually transformed from hepatocytes to progenitor-like cells: ProliHHs-P (Fig. 1B; Supplemental Fig. 1). After four passages, the cell number of ProliHHs could be expanded 200-fold, especially more than 1000-fold in donor MRW (Supplemental Fig. 2).

When the proliferated culture conditions (HM medium/hypoxia) were removed and ProliHHs were transferred to 3D culture plates with HIM, ProliHHs were able to form spheroids and display a well defined shape (Fig. 1B, right), which suggested the maturation of ProliHHs. Meanwhile, the progenitor genes, such as SRY-box transcription factor 17 (*SOX17*) and cytokeratin 7 (*CK7*), were significantly upregulated in ProliHHs-P and returned to levels comparable to PHHs after 3D culture (Fig. 1C). In contrast, the hepatic genes, such as hepatocyte nuclear factor 4 alpha (*HNF4A*), CCAAT/enhancer-binding protein alpha (*CEBPA*), albumin (*ALB*), and alpha-1 antitrypsin (*AAT*), were significantly downregulated in ProliHHs-P and went back to levels comparable to PHHs in ProliHHs-M (Fig. 1, D and E).

To our knowledge, albumin secretion was always used as a functional biomarker of hepatocytes. Being consistent with the gene expression levels, albumin excretion was gradually reduced with serial passages in ProliHHs-P (Fig. 1F) and significantly increased to 3.8 ± 0.1 μg/d per million cells in ProliHHs-M after 8 days of 3D culture comparable to and even better than their original PHHs (Fig. 1F). Together, these results indicated that ProliHHs were able to generate from PHHs and mature after 3D culture.

The Expressions and Metabolic Activities of Three Major P450 Enzymes in ProliHHs. The metabolic capacities of ProliHHs were assessed by gene expressions and probe substrate clearances of selected major DMEs. We first analyzed the expression levels of *CYP1A2*, *CYP2B6*, and *CYP3A4* in ProliHHs-P and found that the expression levels of these genes were downregulated dramatically with serial passage compared with PHHs (Fig. 2A; Supplemental Fig. 3). Similarly, a decrease of metabolic capacity was also observed in ProliHHs-P, but weak metabolic activities were still maintained at passage 4 (Fig. 2B), whereas after the 3D maturation (ProliHHs-M), the expressions and functions of these indicated enzymes recovered significantly. The expression levels of *CYP1A2*, *2B6*, and *3A4* in ProliHHs-M were significantly higher than ProliHHs-P but still less than PHHs (Fig. 2A). The intrinsic clearances of selected P450 substrates also increased significantly (Fig. 2B). The results suggested that ProliHHs-M could achieve the P450 metabolic capacities of their donor PHHs to some extent, especially for CYP1A2 and 3A4 (Fig. 2C). Together, these findings indicated that ProliHHs were able to improve the gene expression and metabolic activities of three major DMEs after 3D culture.

The Metabolic Activities of P450 Enzymes in ProliHHs-M and PHHs. Furthermore, a comparison of metabolic capacities of seven DMEs between ProliHHs-M and their derived PHHs were performed with three independent donors (Fig. 3). Except for CYP2C19, the intrinsic clearances of CYP1A2, 2D6, 3A4, and 2E1 in ProliHHs-M were approximately within 3-fold of PHHs. CYP2B6 and 2C9 enzyme activities were within a 5-fold range compared between ProliHHs-M and PHHs. The ProliHHs-M CL_{int} values of CYP2C19 and 2D6 were above the proportion of PHHs, whereas CYP2B6, 2C9, and 3A4 were below the proportion of PHHs. Together, these data suggested that the ProliHHs-M system may be used to estimate the clearance of major DMEs in their PHH counterparts to some extent.

The Formation of Bile Canalicular Networks in Sandwich-Cultured ProliHHs. According to the preliminary study, ProliHHs can only revert to mature status in a 3D culture environment (e.g., ProliHHs-derived 3D

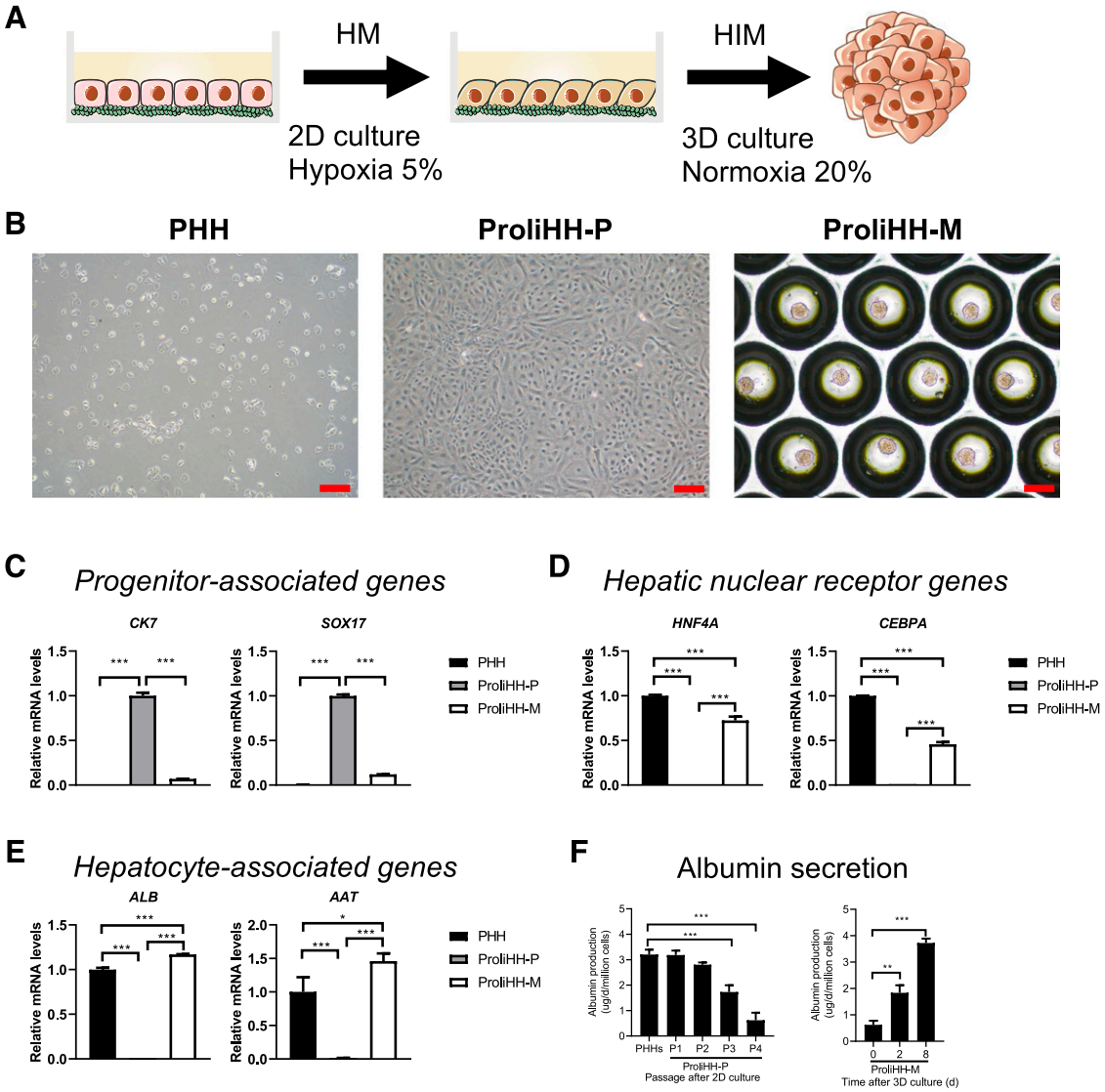

Fig. 1. ProliHHs were proliferative in hypoxia and HM conditions and revert to maturation status in normoxia and 3D culture environment. (A) The schematic overview showed the protocol for proliferation and maturation of ProliHHs. (B) Phase microscopy showed representative morphologies of ProliHHs at days 0, 28, and 38 (after 10-day 3D culture). Scale bars, 100 μm. (C–E) Real-time qPCR analyses of progenitor-associated genes CK7 and SOX17 (C), hepatic nuclear receptor genes CEBPA and HNF4A (D), and secretion protein genes AAT and ALB (E) in PHHs and ProliHHs ($n = 3$). CK7 and Sox17 were normalized to ProliHHs-P, and others were normalized to PHHs. (F) Albumin secretion in ProliHHs-P at indicated passages and in ProliHHs-M at days 0, 2, and 8. ProliHHs were derived from donor QIE. All error bars indicate ±S.D. $^{*}P < 0.05$; $^{**}P < 0.01$; $^{***}P < 0.001$.

organoids) (Zhang et al., 2018). However, 3D organoids are not suitable for quantitative transporter studies. Therefore, a sandwich-culture model was employed to evaluate if ProliHHs could form canalicular networks after sandwich culture.

The sandwich-culture strategy is illustrated in Fig. 4A. Typically, ProliHHs-P or ProliHHs-M were trypsinized and then sandwich-cultured in 24-well plates. SC-PHHs, cultured for 5 days, were used as a positive control. After sandwich culture for 7 days, cell morphology, bile canaliculi structure, and cell polarization of ProliHHs were investigated. Sandwich-cultured ProliHHs-M (SC-ProliHHs-M) exhibited good hepatocyte-like morphology, including cubical shape, tight junctions, and bile canalicular-like structures, whereas the hepatocyte-like cell appearance in sandwich-cultured ProliHHs-P (SC-ProliHHs-P) was not as obvious as in SC-ProliHHs-M (Fig. 4B). Both SC-ProliHHs-P and SC-ProliHHs-M were able to form bile canalicular networks, evidenced by fluorescent dye (Fig. 4C).

Furthermore, the expression levels of essential uptake/efflux transporters were investigated for cells derived from both ProliHHs systems. First, real-time qPCR results showed the expression levels of these transporters were downregulated significantly in ProliHHs-P but significantly upregulated in ProliHHs-M (Fig. 5A). To examine efflux transporter functions, such as BSEP and MRP2, sandwich-cultured cells were incubated with their substrates (CLF and d8-TCA for BSEP, CDF and rosuvastatin for MRP2). Although the expression levels of these genes in ProliHHs-P were rarely detected than PHHs, all the tested compounds showed biliary excretion trends in ProliHHs-P (BEI values >10%). For SC-ProliHHs-M, the BEI values of tested compounds were increased or even comparable to PHHs (Fig. 5B). Together, these findings suggested that ProliHHs in sandwich-culture could maintain polarity, form bile canaliculi networks, and display biliary excretion capacity.

Hepatotoxicity Assessment in ProliHHs. To further investigate whether ProliHHs can be used to evaluate drug-induced hepatotoxicity,

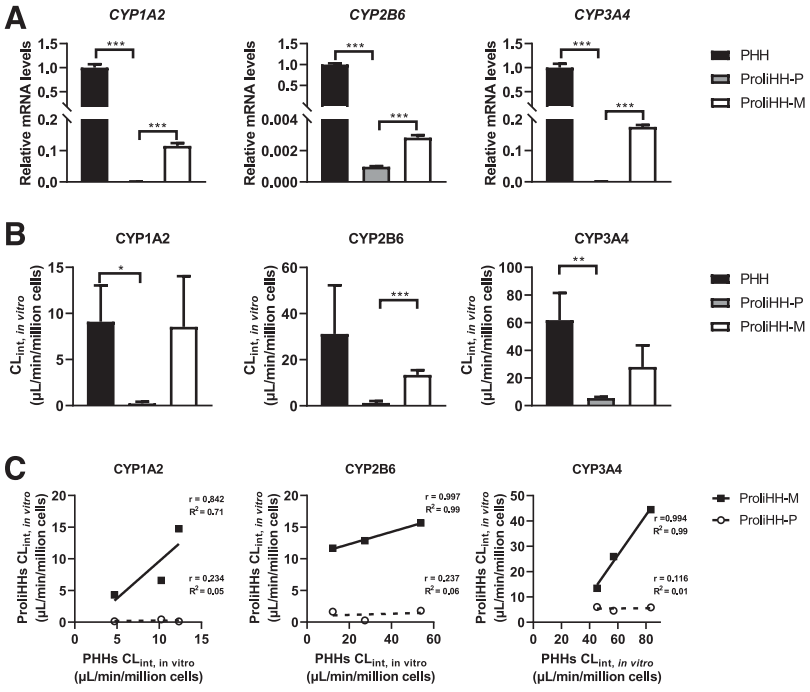

Fig. 2. ProliHHs-M showed P450 expression, enzyme function similar to those of PHHs. (A) Comparison of P450 mRNA expression determined at PHHs, ProliHHs-P (proliferative status, passage 4), and ProliHHs-M (maturation status) from donor QIE by qPCR. (B) Comparison of P450 enzyme activities of PHHs, ProliHsH-P, and ProliHHs-M. CYP1A2, 2B6, and 3A4 measured by phenacetin, bupropion, and testosterone, respectively. ProliHHs were derived from donors MRW, 17905A, and 15101. (C) Comparison of in vitro clearance rates of phenacetin, bupropion, and testosterone measured in ProliHHs-P and ProliHHs-M with their native PHHs source. ProliHHs were derived from donor MRW, 17905A, and 15101. All error bars indicate ±S.D. The correlation between groups was evaluated by the Pearson correlation coefficient (r). $*P < 0.05$; $**P < 0.01$; $***P < 0.001$.

12 compounds were selected to perform 24-hour acute toxicity assessment. The TC_{50} values of three compounds (rifampicin, isoniazid, and valproic acid) in PHHs were from reported literature (Supplemental Table 4). Both ProliHHs-P and ProliHHs-M responded to these drugs in 24 hours and displayed good correlation with PHHs (Fig. 6, A and B). Compared with PHHs, the 2D culture system gave a much higher TC_{50} estimation for imipramine and tamoxifen approximately above 3-fold (Fig. 6A), whereas the TC_{50} value of troglitazone and imipramine in ProliHHs-M was much higher than PHHs (Fig. 6B). When TC_{50} values were compared with PHHs, the AAFE was 1.27 and 2.13 for ProliHHs-P and ProliHHs-M, respectively. Together, these results demonstrated that both ProliHHs-M and ProliHHs-P could be an alternative hepatocyte model for PHHs in drug cytotoxicity evaluation. Considering the cost and convenience, ProliHHs-P should be a better choice for early discovery drug screening phase.

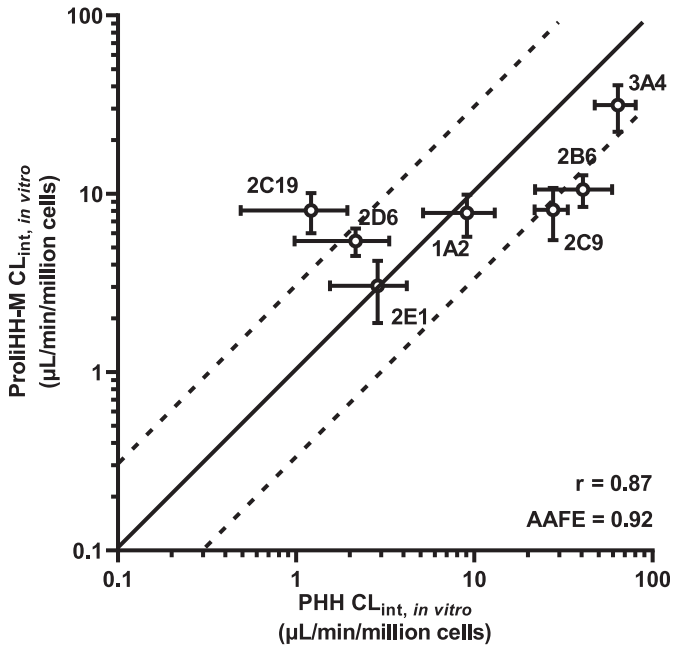

Fig. 3. Comparison of P450 metabolic capacities between ProliHHs-M and PHHs. Correlation of absolute enzyme activity levels determined in ProliHHs-M and PHHs for CYP1A2, CYP2B6, CYP3A4, CYP2C19, CYP2D6, CYP2C9, and CYP2E1. All error bars indicate ±S.E.M. Clearance measured in ProliHHs-M from donors MRW, 17905A, and 15101. The correlation between ProliHHs-M and PHHs was evaluated by the AAFE. The solid and dashed lines represent conformity and 3-fold error range, respectively.

Discussion

A variety of hepatocyte models, such as embryonic stem cell– or induced pluripotent stem cell–derived hepatocyte-like cells, human induced hepatocytes, HepaRG cells, and UHHs, have been developed to study drug metabolism, transport, and drug-induced liver injury (DILI) (McGill et al., 2011; Levy et al., 2015; Ni et al., 2016; Bell et al., 2017). However, these hepatocyte models for application are limited by the lack of physiologic relevance or donor variability (Brolén et al., 2010; Katsuda et al., 2012; Huang et al., 2014). For example, the transcripts of major DMEs in UHHs still need to be improved at donor-specific levels (Levy et al., 2015; Schaefer et al., 2016). It is vital to develop new promising cell models that address these issues. Recently, with the help of dedifferentiation strategy, PHHs could be expanded, display biphenotypic and stable genetic characteristics, and also could be converted back to mature "hepatocytes" after 3D culture (Zhang et al., 2018). Compared with PHHs, the advantages of ProliHHs include low cost, ease of obtaining, diversified donor background, etc. However, it is not clear if it is feasible to evaluate drug metabolism, biliary excretion, and toxicity, especially from the transport aspect, using this novel cell model. Therefore, in this paper, for the first time, the drug metabolic capacities and efflux transporter functions of ProliHHs, as well as their potential in toxicity assessments, were fully characterized.

According to the previous study, ProliHHs could be expanded up to 10,000-fold at passage 8 from young PHH donor cells (Zhang et al., 2018). In this study, the total cell number of ProliHHs was enlarged more than 200-fold at passage 4, which is enough for the following studies, and no further proliferation test was performed (Supplemental Fig. 2).

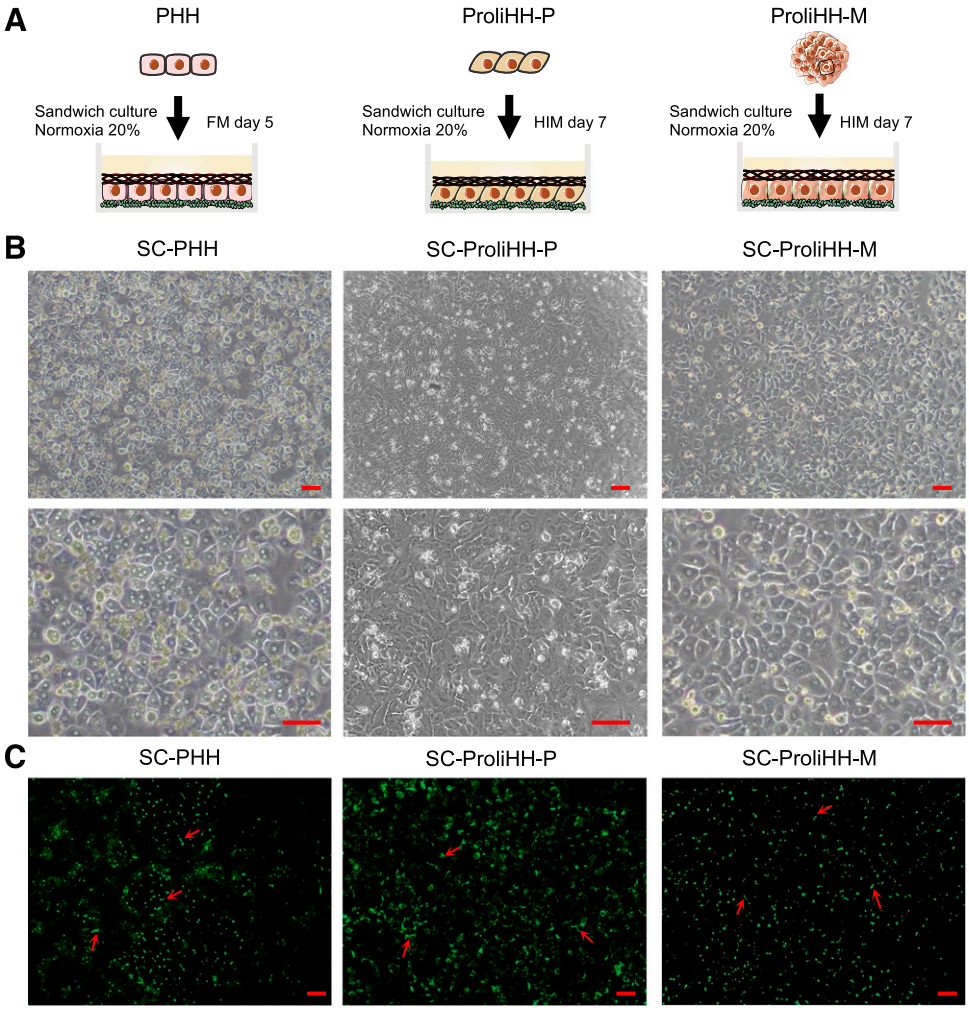

Fig. 4. Bile canaliculi formation and polarization of ProliHHs. (A) The schematic overview showed the protocol for sandwich culture of PHHs, ProliHHs-P, and ProliHHs-M. FM, feeding medium. (B) Phase microscopy showed morphology of SC-ProliHHs-M similar to SC-PHHs. (C) CDFDA staining: CDFDA fluorescence intensity tends to converge to the junction of ProliHHs. The bile canaliculi structure is marked with a red arrow. ProliHHs were derived from donor MRW. Scale bars, 100 μm.

These results are consistent with previous reporting that PHHs will lose their hepatic phenotype and metabolic capacity rapidly during in vitro culture (Gómez-Lechón et al., 2014), and the 3D scaffold culture system could preserve the P450 gene expression and hepatocyte-specific functions for PHHs (Schaefer et al., 2016; Heslop et al., 2017; Bell et al., 2018). These data indicated that ProliHHs from different donors

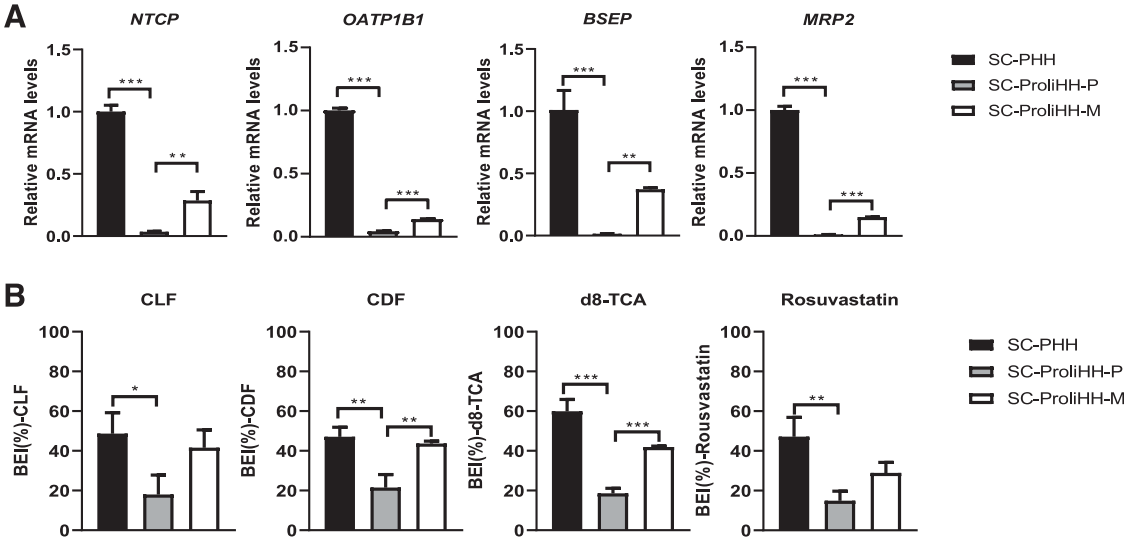

Fig. 5. Transporter expression and function of ProliHHs in sandwich culture system. (A) Real-time qPCR analyses of major transporter genes (NTCP, OATP1B1, BSEP, and MRP2) in ProliHHs at indicated stages, gene expressions are normalized to SC-PHHs. (B) Four different compounds were used to determine the BEI of SC-PHHs and SC-ProliHHs. ProliHHs were generated from donor MRW. $*P < 0.05$; $**P < 0.01$; $***P < 0.001$.

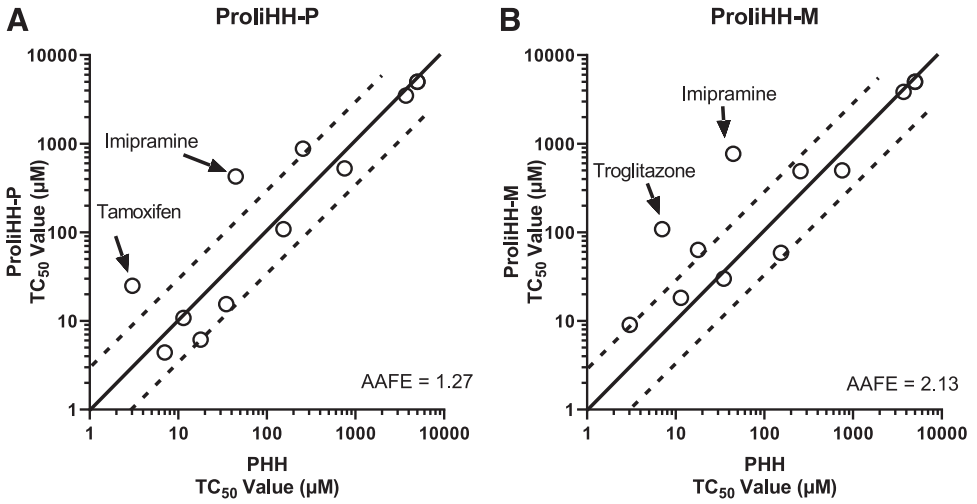

Fig. 6. Comparable toxicity prediction ability of ProliHHs with PHHs. (A) Comparison of the TC_{50} values in PHHs and ProliHHs-P with 12 compounds. (B) Comparison of the TC_{50} values in PHHs and ProliHHs-M with 12 compounds. ProliHHs were derived from donor 15101. The solid and dashed lines represent conformity and 3-fold error range, respectively. The TC_{50} values in both PHHs and ProliHHs higher than 5000 μM was marked as 5000 μM in the figure.

gradually lost hepatic functions with serial passages and regained primary hepatocyte appearances and functions after 3D culture.

The loss of the phenotype of hepatocytes and the increase of the phenotype of liver progenitors were observed during the proliferating process of ProliHHs (Fig. 1, C–E; Supplemental Fig. 3). The expression of major DMEs and transporters also rapidly declined in ProliHHs-P (Fig. 2A; Fig. 5A), which was common for the dedifferentiation process (Kim et al., 2018; Zhang et al., 2018; Fu et al., 2019). The phenotypes of PHHs could be regained in ProliHHs-M after 3D culture, for instance, the improvement of metabolic capacity given the fact that ProliHHs-M were more flexible to predict intrinsic clearances of DMEs (Fig. 2, B and C; Fig. 3). The intrinsic clearances of selected P450 substrates in ProliHHs-M were able to predict the CL_{int} ranking of their PHH donors to some extent (Fig. 2C). These results indicated that the metabolic variabilities in different donors (interindividual variability) could be inherited by their derived ProliHHs, respectively, and the donor specific functions could be rebuilt in a short term.

It is worthwhile to note that although mRNA expression of P450 enzymes in ProliHHs-M is much less than that in PHHs, metabolic activity mediated by these enzymes in ProliHHs-M was close to that in PHHs. For example, CYP2B6 mRNA level in ProliHHs-M was about 1/300 as much as that in PHHs, whereas its CL_{int} was about one-third of PHHs (Fig. 2, A and B). To clarify this disconnection, the protein expression level of CYP2B6 in ProliHHs-M and PHHs was determined by Western blotting. It was found that although the mRNA level of CYP2B6 in ProliHHs was about 1/300 in PHHs, its protein level was comparable to PHHs (~one-third of PHHs) (Supplemental Fig. 4). This disconnection could partially be attributed to the post-transcriptional process of these related genes and the different half-life of mRNA and protein (Berger et al., 2016).

In addition, ProliHHs-M were more efficient as an alternative hepatocyte model for drug metabolic investigation with donor-specific character compared with ProliHHs-P (Fig. 2C). Based on it, the functional comparison of seven major DMEs between ProliHHs-M and PHHs indicated ProliHHs-M could predict intrinsic clearances of these DMEs in PHHs successfully. A positive correlation (r = 0.87) was found, and four DMEs of the CL_{int} values were within 3-fold (AAFE = 0.92) accuracy (Fig. 3). Especially, a good prediction of CYP2E1 was displayed in ProliHHs-M, which may be attributed to their higher mRNA expression level as previously reported (Zhang et al., 2018). The higher CYP2C19 activity (above 3-fold accuracy range) in ProliHHs-M may be attributed to dexamethasone (CYP2C19 inducer) added in HIM (Raucy et al., 2002). However, because ProliHHs-M are different from HepaRG cells and UHHs, the expression and function of CYP2B6 in ProliHHs-M was lower than PHHs, which might be associated with suboptimal 3D culture conditions (without dimethylsulfoxide or FGF19 in HIM) (Kanebratt and Andersson, 2008; Schaefer et al., 2016). Therefore, further manipulation of the culture system will be required to generate more functional ProliHHs-M that are capable of efficiently replacing PHHs for drug metabolic studies.

Sinusoidal and canalicular transport properties are critical for primary hepatocytes. The lack of uptake and efflux transporter functions limits various alternative hepatocyte models in the preclinical evaluation of DILI and cholestasis (Donato et al., 2013; Bell et al., 2016; Zhang et al., 2016). Previous studies reported that CDFDA has been commonly used to study the function of efflux transporters, e.g., MRP2 (Anthérieu et al., 2010; Levy et al., 2015). In this study, we found that ProliHHs could be polarized in sandwich culture, which was essential for the proper efflux of bile acids or toxic drugs, and both cells from proliferative and maturation status of ProliHHs could form canalicular networks in sandwich culture (Fig. 4, B and C). Furthermore, compounds that may lead to cholestasis were investigated for their potential DILI risk using SC-ProliHHs. To evaluate the BSEP efflux function, d8-TCA was selected to assess the efflux transporter functions in SC-ProliHHs (Fig. 5B). Three selected cholestatic drugs (rifampin, glibenclamide, and ketoconazole) were reported as the inhibitors of BSEP (Ni et al., 2016; Wu et al., 2016). In this study, all of them significantly inhibited d8-TCA biliary excretion in SC-ProliHHs-P (Supplemental Fig. 5). Of course, the sandwich-cultured cells derived from ProliHHs-M displayed higher BEI values than ProliHHs-P, which were close to the BEI values of PHHs (Fig. 5B). However, considering the timing and cost of 3D culture, SC-ProliHHs-P were a better choice for the early drug discovery stage. More comprehensive studies, including organic anion-transporting polypeptide/sodium-taurocholate cotransporting polypeptide uptake and multidrug resistance gene 1 (MDR1) (P-glycoprotein) efflux function, are required to fully characterized in SC-ProliHH in the future.

The evaluation of drug hepatotoxicity is essential for preclinical drug safety study (Donato et al., 2013; Sebastian et al., 2014; Zhang et al., 2016). In this study, to investigate whether ProliHHs can be used to evaluate drug-induced cytotoxicity, 12 compounds were selected to perform acute toxicity assessment. All tested compounds covered a broad toxicity dose range (TC_{50} ranged from 1 to 5000 μM) with varied liver toxic mechanisms, for example, metabolic activation (chenodeoxycholic acid, ibuprofen, and isoniazid), cholestasis (lithocholic acid, chlorpromazine, and imipramine), reactive oxygen species (cyclosporin A, rifampin, amiodarone, and valproic acid), and multiple

mechanisms (troglitazone and tamoxifen) (Wang et al., 2002; Kemp and Brouwer, 2004; Ni et al., 2016; Xie et al., 2019). In most cases, the TC_{50} values of the selected compounds in both ProliHHs-M and ProliHHs-P were within 3-fold accuracy with those in PHHs (Fig. 6, A and B). The higher TC_{50} values of tamoxifen in ProliHHs-P may be attributed to the low expression of uptake transporter organic anion-transporting polypeptide 1B1 during the proliferating process (Fig. 5A) (Gao et al., 2017), whereas the higher TC_{50} value of troglitazone in ProliHHs-M may be attributed to the increasing function of DMEs (CYP2C19, CYP2D6, and CYP3A4) and efflux transporters (BSEP and MRP2) in ProliHHs-M (Fig. 3; Fig. 5B) (Mueller et al., 2014). In addition, both ProliHHs-P and ProliHHs-M were insensitive to imipramine, for which liver toxicity was related to the production of metabolic intermediates (Lemoine et al., 1993; Su et al., 1993). We attributed these to the lower functions of related metabolic enzymes compared with their PHHs counterparts. Together, these results showed that both of 3D cultured ProliHHs-M spheroids and ProliHHs-P were able to predict transporter mediated cytotoxicity, and ProliHHs-P could be used to assess drug cytotoxicity in a quick, convenient, and efficient way.

In conclusion, the proliferative and maturation protocol of ProliHHs were fully characterized from perspectives of metabolic enzyme and transporter. The metabolic capacities of 3D cultured ProliHHs-M are comparable to PHHs. The sandwich-cultured ProliHHs recovered and maintained transporter function for biliary excretion and cholestasis risk assessment. Both ProliHHs-P and ProliHHs-M could be used to evaluate cytotoxicity. ProliHHs-P have the potential to be developed into a screening tool to detect cytotoxicity. Therefore, a novel strategy combining 3D and sandwich culture makes it feasible for ProliHHs to support drug candidate screening in hepatic metabolism, disposition, and toxicity.

Acknowledgments

We thank Yaru Xue, Ying Wang, and Xin Luo for technical support with hepatocyte culture, as well as Kun Zhang, Chenhua Wang, Ludi Zhang, and Lijian Hui for greatly supporting this work. Both proliferative and maturation medium components of ProliHHs were kindly provided by Prof. Lijian Hui. Trypsinized ProliHHs-M were gifted by Ludi Zhang for sandwich culture.

Authorship Contributions

Participated in research design: Qiao, Feng, Tian, Pan.
Conducted experiments: Qiao, Feng, He, Ma, Peng.
Performed data analysis: Qiao, Feng, Wu, He, Ma.
Wrote or contributed to the writing of the manuscript: Qiao, Feng, Wu, Pan.

References

Andersson TB, Kanebratt KP, and Kenna JG (2012) The HepaRG cell line: a unique in vitro tool for understanding drug metabolism and toxicology in human. *Expert Opin Drug Metab Toxicol* **8**:909–920.

Anthérieu S, Chesné C, Li R, Camus S, Lahoz A, Picazo L, Turpeinen M, Tolonen A, Uusitalo J, Guguen-Guillouzo C, et al. (2010) Stable expression, activity, and inducibility of cytochromes P450 in differentiated HepaRG cells. *Drug Metab Dispos* **38**:516–525.

Bell CC, Dankers ACA, Lauschke VM, Sison-Young R, Jenkins R, Rowe C, Goldring CE, Park K, Regan SL, Walker T, et al. (2018) Comparison of hepatic 2D sandwich cultures and 3D spheroids for long-term toxicity applications: a multicenter study. *Toxicol Sci* **162**:655–666.

Bell CC, Hendriks DF, Moro SM, Ellis E, Walsh J, Renblom A, Fredriksson Puigvert L, Dankers AC, Jacobs F, Snoeys J, et al. (2016) Characterization of primary human hepatocyte spheroids as a model system for drug-induced liver injury, liver function and disease. *Sci Rep* **6**:25187.

Bell CC, Lauschke VM, Vorrink SU, Palmgren H, Duffin R, Andersson TB, and Ingelman-Sundberg M (2017) Transcriptional, functional, and mechanistic comparisons of stem cell–derived hepatocytes, HepaRG cells, and three-dimensional human hepatocyte spheroids as predictive in vitro systems for drug-induced liver injury. *Drug Metab Dispos* **45**:419–429.

Berger B, Donzelli M, Maseneni S, Boess F, Roth A, Krähenbühl S, and Haschke M (2016) Comparison of liver cell models using the basel phenotyping cocktail. *Front Pharmacol* **7**:443.

Brolén G, Sivertsson L, Björquist P, Eriksson G, Ek M, Semb H, Johansson I, Andersson TB, Ingelman-Sundberg M, and Heins N (2010) Hepatocyte-like cells derived from human embryonic stem cells specifically via definitive endoderm and a progenitor stage. **145**:284–294.

Donato MT, Jover R, and Gómez-Lechón MJ (2013) Hepatic cell lines for drug hepatotoxicity testing: limitations and strategies to upgrade their metabolic competence by gene engineering. *Curr Drug Metab* **14**:946–968.

Fu G-B, Huang W-J, Zeng M, Zhou X, Wu H-P, Liu C-C, Wu H, Weng J, Zhang H-D, Cai Y-C, et al. (2019) Expansion and differentiation of human hepatocyte-derived liver progenitor-like cells and their use for the study of hepatotropic pathogens. *Cell Res* **29**:8–22.

Gao C-M, Pu Z, He C, Liang D, Jia Y, Yuan X, Wang G, and Xie H (2017) Effect of OATP1B1 genetic polymorphism on the uptake of tamoxifen and its metabolite, endoxifen. *Oncol Rep* **38**: 1124–1132.

Godoy P, Hewitt NJ, Albrecht U, Andersen ME, Ansari N, Bhattacharya S, Bode JG, Bolleyn J, Borner C, Böttger J, et al. (2013) Recent advances in 2D and 3D in vitro systems using primary hepatocytes, alternative hepatocyte sources and non-parenchymal liver cells and their use in investigating mechanisms of hepatotoxicity, cell signaling and ADME. *Arch Toxicol* **87**: 1315–1530.

Gómez-Lechón MJ, Donato MT, Castell JV, and Jover R (2003) Human hepatocytes as a tool for studying toxicity and drug metabolism. *Curr Drug Metab* **4**:292–312.

Gómez-Lechón MJ, Donato MT, Castell JV, and Jover R (2004) Human hepatocytes in primary culture: the choice to investigate drug metabolism in man. *Curr Drug Metab* **5**:443–462.

Gómez-Lechón MJ, Tolosa L, Conde I, and Donato MT (2014) Competency of different cell models to predict human hepatotoxic drugs. *Expert Opin Drug Metab Toxicol* **10**:1553–1568.

Guo C, He L, Yao D, A J, Cao B, Ren J, Wang G, and Pan G (2014) Alpha-naphthylisothiocyanate modulates hepatobiliary transporters in sandwich-cultured rat hepatocytes. *Toxicol Lett* **224**: 93–100.

Heslop JA, Rowe C, Walsh J, Sison-Young R, Jenkins R, Kamalian L, Kia R, Hay D, Jones RP, Malik HZ, et al. (2017) Mechanistic evaluation of primary human hepatocyte culture using global proteomic analysis reveals a selective dedifferentiation profile. *Arch Toxicol* **91**:439–452.

Hewitt NJ, Lechón MJ, Houston JB, Hallifax D, Brown HS, Maurel P, Kenna JG, Gustavsson L, Lohmann C, Skonberg C, et al. (2007) Primary hepatocytes: current understanding of the regulation of metabolic enzymes and transporter proteins, and pharmaceutical practice for the use of hepatocytes in metabolism, enzyme induction, transporter, clearance, and hepatotoxicity studies. *Drug Metab Rev* **39**:159–234.

Huang P, Zhang L, Gao Y, He Z, Yao D, Wu Z, Cen J, Chen X, Liu C, Hu Y, et al. (2014) Direct reprogramming of human fibroblasts to functional and expandable hepatocytes. *Cell Stem Cell* **14**:370–384.

Kanebratt KP and Andersson TB (2008) Evaluation of HepaRG cells as an in vitro model for human drug metabolism studies. *Drug Metab Dispos* **36**:1444–1452.

Katsuda T, Sakai Y, and Ochiya T (2012) Induced pluripotent stem cell-derived hepatocytes as an alternative to human adult hepatocytes. *J Stem Cells* **7**:1–17.

Kemp DC and Brouwer KL (2004) Viability assessment in sandwich-cultured rat hepatocytes after xenobiotic exposure. *Toxicol In Vitro* **18**:869–877.

Kim Y, Kang K, Lee SB, Seo D, Yoon S, Kim SJ, Jang K, Jung YK, Lee KG, Factor VM, et al. (2018) Small molecule-mediated reprogramming of human hepatocytes into bipotent progenitor cells. *J Hepatol* **70**:97–107.

Kimoto E, Bi Y-A, Kosa RE, Tremaine LM, and Varma MVS (2017) Hepatobiliary clearance prediction: species scaling from monkey, dog, and rat, and In Vitro-In Vivo extrapolation of sandwich-cultured human hepatocytes using 17 drugs. *J Pharm Sci* **106**:2795–2804.

Lemoine A, Gautier JC, Azoulay D, Kiffel L, Belloc C, Guengerich FP, Maurel P, Beaune P, and Leroux JP (1993) Major pathway of imipramine metabolism is catalyzed by cytochromes P-450 1A2 and P-450 3A4 in human liver. *Mol Pharmacol* **43**:827–832.

Levy G, Bomze D, Heinz S, Ramachandran SD, Noerenberg A, Cohen M, Shibolet O, Sklan E, Braspenning J, and Nahmias Y (2015) Long-term culture and expansion of primary human hepatocytes. *Nat Biotechnol* **33**:1264–1271.

Liang G and Zhang Y (2013) Genetic and epigenetic variations in iPSCs: potential causes and implications for application. *Cell Stem Cell* **13**:149–159

Liu X, Chism JP, LeCluyse EL, Brouwer KR, and Brouwer KL (1999) Correlation of biliary excretion in sandwich-cultured rat hepatocytes and in vivo in rats. *Drug Metab Dispos* **27**: 637–644.

Ma H, Morey R, O'Neil RC, He Y, Daughtry B, Schultz MD, Hariharan M, Nery JR, Castanon R, Sabatini K, et al. (2014) Abnormalities in human pluripotent cells due to reprogramming mechanisms. *Nature* **511**:177–183.

McGill MR, Yan HM, Ramachandran A, Murray GJ, Rollins DE, and Jaeschke H (2011) HepaRG cells: a human model to study mechanisms of acetaminophen hepatotoxicity. *Hepatology* **53**: 974–982.

Mueller D, Krämer L, Hoffmann E, Klein S, and Noor F (2014) 3D organotypic HepaRG cultures as in vitro model for acute and repeated dose toxicity studies. *Toxicol In Vitro* **28**:104–112.

Ni X, Gao Y, Wu Z, Ma L, Chen C, Wang L, Lin Y, Hui L, and Pan G (2016) Functional human induced hepatocytes (hiHeps) with bile acid synthesis and transport capacities: a novel in vitro cholestatic model. *Sci Rep* **6**:38694.

O'Brien PJ, Irwin W, Diaz D, Howard-Cofield E, Krejsa CM, Slaughter MR, Gao B, Kaludercic N, Angeline A, Bernardi P, et al. (2006) High concordance of drug-induced human hepatotoxicity with in vitro cytotoxicity measured in a novel cell-based model using high content screening. *Arch Toxicol* **80**:580–604.

Ogawa S, Surapisitchat J, Virtanen C, Ogawa M, Niapour M, Sugamori KS, Wang S, Tamblyn L, Guillemette C, Hoffmann E, et al. (2013) Three-dimensional culture and cAMP signaling promote the maturation of human pluripotent stem cell-derived hepatocytes. *Development* **140**: 3285–3296.

Pan G, Boiselle C, and Wang J (2012) Assessment of biliary clearance in early drug discovery using sandwich-cultured hepatocyte model. *J Pharm Sci* **101**:1898–1908.

Petrov PD, Fernández-Murga ML, López-Riera M, Goméz-Lechón MJ, Castell JV, and Jover R (2018) Predicting drug-induced cholestasis: preclinical models. *Expert Opin Drug Metab Toxicol* **14**:721–738.

Ramachandran SD, Vivarès A, Klieber S, Hewitt NJ, Muenst B, Heinz S, Walles H, and Braspenning J (2015) Applicability of second-generation upcyte® human hepatocytes for use in CYP inhibition and induction studies. *Pharmacol Res Perspect* **3**:e00161.

Raucy JL, Mueller L, Duan K, Allen SW, Strom S, and Lasker JM (2002) Expression and induction of CYP2C P450 enzymes in primary cultures of human hepatocytes. *J Pharmacol Exp Ther* **302**: 475–482.

Schaefer M, Schänzle G, Bischoff D, and Süssmuth RD (2016) Upcyte human hepatocytes: a potent in vitro tool for the prediction of hepatic clearance of metabolically stable compounds. *Drug Metab Dispos* **44**:435–444.

Sebastian K, Mueller D, Valery, Schevchenko V, and Noor F (2014) Long-term maintenance of HepaRG cells in serum-free conditions and application in a repeated dose study. *J Appl Toxicol* **34**:1078–1086.

Si-Tayeb K, Noto FK, Nagaoka M, Li J, Battle MA, Duris C, North PE, Dalton S, and Duncan SA (2010) Highly efficient generation of human hepatocyte-like cells from induced pluripotent stem cells. *Hepatology* **51**:297–305.

Su P, Coutts RT, Baker GB, and Daneshtalab M (1993) Analysis of imipramine and three metabolites produced by isozyme CYP2D6 expressed in a human cell line. *Xenobiotica* **23**:1289–1298.

Wang K, Shindoh H, Inoue T, and Horii I (2002) Advantages of in vitro cytotoxicity testing by using primary rat hepatocytes in comparison with established cell lines. *J Toxicol Sci* **27**: 229–237.

Wu Z-T, Yao D, Ji S-Y, Ni X, Gao Y-M, Hui L-J, and Pan G-Y (2016) Optimized hepatocyte-like cells with functional drug transporters directly-reprogrammed from mouse fibroblasts and their potential in drug disposition and toxicology. *Cell Physiol Biochem* **38**:1815–1830.

Xie B, Sun D, Du Y, Jia J, Sun S, Xu J, Liu Y, Xiang C, Chen S, Xie H, et al. (2019) A two-step lineage reprogramming strategy to generate functionally competent human hepatocytes from fibroblasts. *Cell Res* **29**:696–710.

Zhang J, Doshi U, Suzuki A, Chang C-W, Borlak J, Li AP, and Tong W (2016) Evaluation of multiple mechanism-based toxicity endpoints in primary cultured human hepatocytes for the identification of drugs with clinical hepatotoxicity: results from 152 marketed drugs with known liver injury profiles. *Chem Biol Interact* **255**:3–11.

Zhang K, Zhang L, Liu W, Ma X, Cen J, Sun Z, Wang C, Feng S, Zhang Z, Yue L, et al. (2018) In vitro expansion of primary human hepatocytes with efficient liver repopulation capacity. *Cell stem cell* **23**:806–819. e4.

Address correspondence to: Guoyu Pan, Shanghai Institute of Materia Medica, Chinese Academy of Sciences, Haike Rd. 501, Shanghai 201203, China. E-mail gypan@simm.ac.cn

Supplemental Materials

Title

Functional proliferating human hepatocytes: *in vitro* hepatocyte model for drug metabolism, excretion and toxicity

Authors

Shida Qiao, Sisi Feng, Ting He, Zhitao Wu, Chen Ma, Zhaoliang Peng, E Tian and Guoyu Pan

Journal: Drug Metabolism and Disposition

DMD-AR-2020-000275

Supplemental data

Supplemental Table 1. Demographics, supplier and metabolic activity of primary human hepatocytes used for metabolism, disposition and toxicity.

No.	Donor	Supplier	Race	Age	Sex	Thaw viability	CYP isoform (pmol/min/million cells)		
							1A2	2B6	3A4
1	MRW[1]	1	C	11mos	M	85%	15.5	4.62	14.0
2	QIE[1]	1	C	7mos	M	86%	12.5	7.19	11.8
3	LHum15101[2]	2	C	33	M	92%	25.0	8.33	6.67
4	LHuf17905A[2]	2	C	58	F	94%	31.6	6.67	6.67

C: Caucasian; [1)] BioreclamationIVT GmbH (Frankfurt/Main, Germany/Baltimore, MD, USA). Cells were incubated in suspension either for 4 hours at 37°C with the following test substrates: phenacetin (15μM), midazolam (15μM), bupropion (250μM).[2)] XenoTech (Lenexa, KS, USA). Cells were incubated in suspension either for 1 hour at 37°C with the following test substrates: phenacetin (200μM), midazolam (50μM), bupropion (100μM). Metabolite rate of formation was measured in CYP1A2 acetaminophen, CYP2B6 hydroxybupropion, and CYP3A4 1-hydromidazolam.

Supplemental Table 2. HPLC/MS-MS conditions and parameters for CYP450 enzyme activity assays.

CYP450 isoform	Probe Substrate	HPLC column	Flow rate (mL/min)	Q1/Q3 (m/z)	Mode	CE
1A2	Phenacetin	1	0.25	180/110.1	Positive	25
2B6	Bupropion	1	0.25	235.2/86.15	Positive	24
2C9	Diclofenac acid	1	0.25	294.1/250.1	Negative	11
2C19	s-Mephenytoin	1	0.25	219.2/133.9	Positive	21
2D6	Dextromethorphan	1	0.25	271.8/171	Positive	40
2E1	Chlorzoxazone	1	0.25	167.9/132.0	Negative	20
3A4	Testosterone	1	0.25	289.1/97.05	Positive	20

HPLC column: 1 INERTSIL ODS-4 C18 (2.1×100 mm), GL Sciences, Japan

Supplemental Table 3. Primer sequences used for RT-qPCR

Gene	Sequences (Forward, 5' to 3')	Sequences (Reverse, 5' to 3')
CK7	GACATCTTTGAGGCCCAGATT	CTTGAAGTCCTCCACCACATC
SOX17	CTGGTGATGGTTGCACAATTC	CGCCCTTCACCTTCATGT
HNF4A	TCCAACCCAACCTCATCCTCCTTCTT	TCCTCTCCACTCCAAGTTCCTGTT
CEBPA	GATAACCTTGTGCCTTGGAAATG	GAGGCAGGAAACCTCCAAATA
ALB	GTGAAACACAAGCCCAAGGCAACA	TCCTCGGCAAAGCAGGTCTC
AAT	AGGGCCTGAAGCTAGTGGATAAGT	TCTGTTTCTTGGCCTCTTCGGTGT
CYP1A2	ATGCCCTCAACACCTTCTC	CTCCTGCAACCTGCTGAT
CYP2B6	TTGGATGTGTAGAGGACAGAGA	ATACACAGCAAGGCTACAGC
CYP3A4	GTGACCAAATCAGTGTGAGGAGGTAGA	AGGAGGAGTTAATGGTGCTAACTGG
BSEP	TACACAGAGGCGGGTCTATAA	CTGGTCTTCAGTCCTTCTGTTC
MRP2	CCACAAGCCCAGAATAAGGTAG	ACTGACAATTGGTAGGTGAAAGT
NTCP	GTGGCAATCAAGAGTGGTGTC	ACTGGTCCTGGTTCTCATTCC
OATP1B1	TTGGAGGTGTTTTGACTGCTT	ACAAGTGGATAAGGTCGATGTTG
TBP	TTGCTGAGAAGAGTGTGCTGGAGATG	CGTAAGGTGGCAGGCTGTTGTT

Supplemental Table 4. *In vitro* toxicity test TC_{50} values in PHH, ProliHH-P and ProliHH-M for 12 compounds.

Compounds	TC_{50} values (μM)			
	PHH	ProliHH-P	ProliHH-M	literature
Lithocholic acid	153.9	108.7	58.76	
Cyclosporin A	17.87	6.14	63.35	
Troglitazone	7.03	4.41	108.8	
Tamoxifen	3.03	24.94	9.05	
Chlorpromazine	34.83	15.48	30.06	
Amiodarone	11.44	10.83	18.25	
Imipramine	44.43	425.9	770.1	
Chenodeoxycholic Acid	754.7	526.1	500.1	
Ibuprofen	3717	3486	3836	
Valproic acid	>5000 [1]	>5000	>5000	(Albrecht et al., 2019)
Isoniazid	>5000 [1]	>5000	>5000	(Albrecht et al., 2019)
Rifampicin	255 [1]	878.8	488.8	(Albrecht et al., 2019)

Supplemental Figure 1: Morphology of ProliHH at indicated days in HM culture.

Phase microscopy shows colonies of ProliHH generated from primary hepatocytes in day 1, day 3, and day 14. ProliHH were derived from donor QIE. Scale bar, 100 μm.

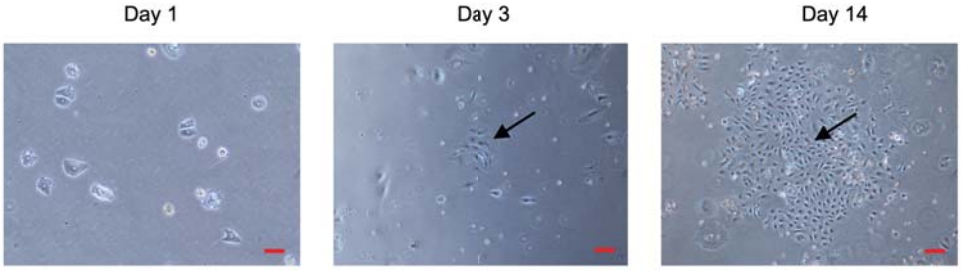

Supplemental Figure 2: ProliHH were proliferative in HM culture.

Growth curves of cultured ProliHH were analyzed at indicated passages.

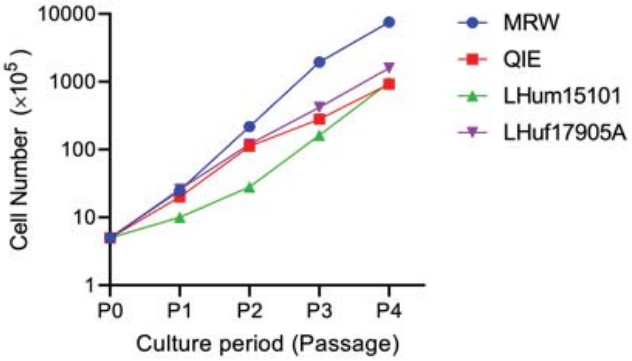

Supplemental Figure 3: Impact of culture time on CYP450 mRNA expression in ProliHH.

Comparison of CYP450 mRNA expression determined at PHH (freshly thawed PHH source) to P4 (week four) of ProliHH-P (donor QIE) by qPCR. (A) CYP1A2 (B) CYP2B6 (C) CYP3A4. Data were normalized to PHH. All error bars indicate ± SD.

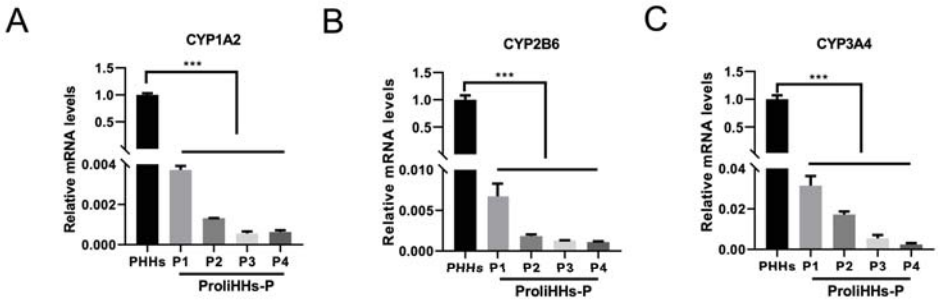

Supplemental Figure 4: Protein expression level of CYP2B6 enzyme in ProliHH-M.

Protein expression level of CYP2B6 enzyme in ProliHH-M was analyzed by Western blotting compared with the PHH. (A) The Western blotting results of CYP2B6 expression in ProliHH-M and PHH (B) The statistical analysis for (A).

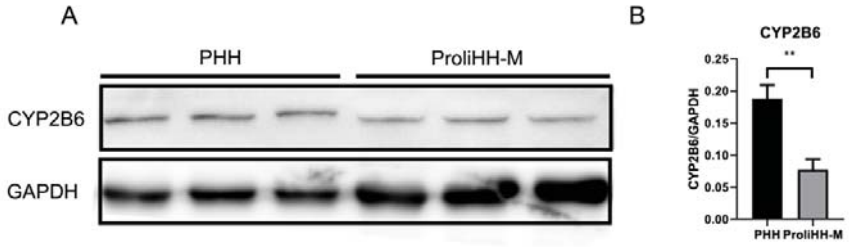

Supplemental Figure 5: Effect of cholestatic drugs on d8-TCA efflux in sandwich cultured ProliHH. SC-ProliHH-P were treated with 5 µM d8-TCA alone or in combination with BSEP inhibitors for 15 min. BSEP inhibitors include 25 µM rifampicin, 10 µM glibenclamide and 30 µM ketoconazole. ProliHH were generated from donor LHum15101.

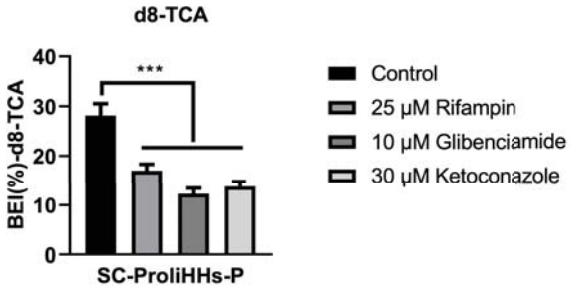

References

Albrecht W, Kappenberg F, Brecklinghaus T, Stoeber R, Marchan R, Zhang M, Ebbert K, Kirschner H, Grinberg M, and Leist M (2019) Prediction of human drug-induced liver injury (DILI) in relation to oral doses and blood concentrations. Archives of toxicology 93:1609-1637.